Chain-Order Effects in Polymer Melts Probed by ^{1}H Double-Quantum NMR Spectroscopy

R. Graf, A. Heuer, and H. W. Spiess
Max-Planck Institut für Polymerforschung, Postfach 3148, D-55021 Mainz, Germany

(Received 2 September 1997)

Double-quantum NMR experiments are presented, elucidating the nature of the polymer chain dynamics in a polybutadiene melt far above the glass transition. The obtained experimental information about the rotational dynamics of spin pairs allows the translational dynamics as well as the long-term stability of the topological constraints on a microscopic scale to be probed. The results are shown to support some but not all aspects of the reptation model. For short times, the local chain order reflecting the time averaged configurations is much larger than expected, indicating strong packing effects. [S0031-9007(98)06506-5]

PACS numbers: 61.25.Hq, 66.20.+d, 81.05.Kf

The dynamics of polymer chains in the melt is a very complicated multibody problem, yet simple models account for many experimental observations, e.g., the Rouse model [1,2] and the reptation model of a tube in which the tagged chain can reptate [2,3]. On the basis of the latter as well as alternative theories [4], observables like the time dependence of the mean-square displacement of chain segments, $\langle \Delta r^2(t) \rangle$, can be analyzed, yielding similar results.

Elucidation of the nature of the complex polymer dynamics on a molecular level is of major importance for understanding the behavior of polymeric materials. Neutron scattering [5,6], NMR spectroscopy (see, e.g., [7–9]) as well as computer simulations [10] yield important insight. Recently, informative ^{1}H-NMR dipolar echo experiments have been performed on poly(dimethyl siloxane) (PDMS) melts [9], extending earlier work on polyethylene [11], in which the dipolar frequency ω_d of proton pairs is monitored. For a given spin pair $\omega_d = P_2(\cos\theta)\delta_d$, where δ_d depends on the distance between both spins and θ denotes their orientation with respect to the external magnetic field. P_2 is the second Legendre polynomial. Hence, information about the rotational dynamics can be obtained by monitoring ω_d [12]. Introducing the phase $\phi(t_1, t_2) \equiv \int_{t_1}^{t_2} d\tau\, \omega_d(\tau)$ acquired during the interval $t_1 < t < t_2$ the experimentally observable function

$$\beta(2t, t) \equiv \langle \sin\phi(0, t) \sin\phi(t, 2t) \rangle \tag{1}$$

has been analyzed. For later convenience we note that for short times and for a broad distribution of correlation times it can be approximated as $t^2\langle \omega_d(0)\omega_d(t) \rangle$ [13]. On short time scales the polymer chain performs fast local dynamical processes. Following the ideas by Cohen Addad [14], for a tagged segment its two closest entanglements serve as a constraint for this dynamics, impeding isotropic dynamics. On time scales much longer than the α-relaxation time but much shorter than the Rouse time t_r this leads to a residual chain order [9,14]. This local anisotropy of the dynamics can be quantified by the *residual order parameter S* by which the effective dipolar coupling is reduced, i.e., $\beta(2t, t) = 0.2S^2\delta_d^2 t^2$, the numerical factor resulting from the isotropic powder average.

As discussed in Refs. [9,11] this function also contains information about the *translational* dynamics of the polymer which the chain performs on somewhat longer time scales. Then a tagged segment will leave its initial environment and the observed spin pairs will acquire a random orientation [9,11]. This leads to a further reduction of $\beta(2t, t)$ which for future purposes is quantified by the function $C(t/t_e)$

$$\beta(2t, t) = 0.2S^2\delta_d^2 t^2 C(t/t_e), \tag{2}$$

with some time scale t_e (see below). NMR spectroscopy, therefore, can provide information about two different aspects of the complex dynamics behavior of polymer chains in the melt: (i) the short time *rotational* motion probing the local constraints free of model assumptions and (ii) the long time *translational* motion.

In this Letter we analyze the dynamics of three different polybutadiene (PB) samples (50%:45%:5% trans:cis:vinyl, $T_g = 174$ K) with molecular weights M_w beyond the entanglement molecular weight ($M_w = ZM_e$; $Z = 4, 11, 76$) via high-resolution homonuclear ^{1}H double-quantum NMR [15]. In addition to measuring the β function presented above our approach provides new information not accessible so far: (i) The spectroscopic resolution of different H-H spin pairs allows the influence of local constrains on the main chain order to be probed quantitatively. (ii) The correlation function $C(t/t_e)$ is determined for four orders of magnitude of t/t_e as compared to one in [9].

For optimum information about the chain dynamics one would like to monitor the order along the main chain of the polymer. The dipolar coupling, however, is due to proton pairs, which are typically *not* aligned along the main chain. However, from simple geometric considerations as well as from appropriate simulations the main chain order, i.e., the order of the C═C bonds, may be inferred from the experimentally accessible order if several H-H pairs in the repeat unit are monitored individually. This renders the results much more reliable. As distinct from the dipolar echo technique [9], this selectivity can now be achieved by

0031-9007/98/80(26)/5738(4)$15.00

high resolution double-quantum NMR spectroscopy under magic angle spinning (MAS) [16].

All double-quantum spectra are recorded in two dimensional (2D) experiments [17], according to the experimental scheme in Fig. 1. After the preparation of the double-quantum coherences in the excitation time t_{exc}, the coherences evolve during t_1 under the residual dipolar coupling. In the reconversion period also of duration t_{exc}, the double-quantum coherences are transformed into longitudinal magnetization and after a 90° pulse the free induction decay (FID) is acquired. A four step phase cycle is used to select the double-quantum signal. The double-quantum part of the dipole-dipole interaction averaged by MAS is reintroduced during the excitation and the reconversion time [18]. As distinct from related techniques, the 2D spectrum under fast MAS only contains contributions from dipolar coupled spin pairs.

The 2D double-quantum spectrum correlates the chemical shifts of both spins forming the pair with the chemical shift of the double-quantum coherence, corresponding to the sum of the chemical shifts. Using an appropriate scaling, signals on the diagonal result from coherences of spins with like chemical shifts, whereas coherences of spins with different shifts appear symmetrically to this diagonal at the spectral positions of both spins involved. In the ^{1}H double-quantum spectrum of PB the aliphatic and the olefinic protons are resolved and all possible coherences ($-CH_2$, CH_2-CH, $CH=CH$) are observed; see Fig. 1. Relative dipolar coupling strengths can be directly obtained from the intensities of the different peaks in the 2D spectrum by individually fitting the intensities $I(t_{\mathrm{exc}})$ via $I = AS_i^2 \delta_{d,i}^2 t_{\mathrm{exc}}^2 \exp(-t_{\mathrm{exc}}/t_0)$ for all resonances i, where A combines all experimental factors. The exponential term accounts for relaxation processes. An example of such a buildup curve is shown in Fig. 2(a). Since $\delta_{d,i}$ is given by the distance between the protons of pair i the product AS_i^2 can be determined for each H-H pair which can be distinguished in the spectrum. For $S_{\mathrm{CH=CH}}$ it was necessary to average the distance over the cis- and the trans-configuration and for $S_{\mathrm{CH_2-CH}}$ over the different distances of both protons according to the rotational isomeric state (RIS) statistics of PB (see below) [19]. From the build-up behavior the *relative* values for the order parameters $S_{\mathrm{CH=CH}}{:}S_{\mathrm{CH_2-CH}}{:}S_{\mathrm{-CH_2}} =$ 1:0.6:0.45 are directly obtained. At the highest temperature ($T = 298$ K), the NMR signals of the trans- and the cis-configuration of the sample are resolved in the double-quantum spectrum and the relative couplings can be measured separately for both configurations; see Fig. 1. From this we estimate $S_{\mathrm{C=C,trans}} \approx 2S_{\mathrm{C=C,cis}}$.

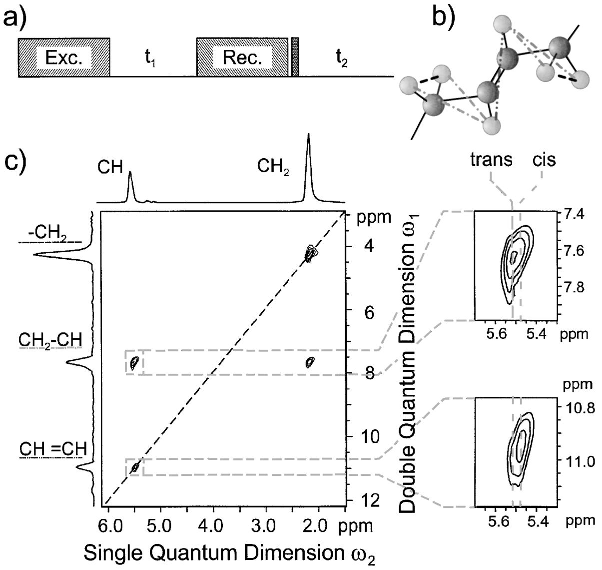

FIG. 1. The experimental scheme (a) is used to measure a high resolution ^{1}H double-quantum spectrum ($\omega_{L,^1\mathrm{H}} =$ 500 MHz) of 1,4-polybutadiene ($M_W = 130\,000$ g/mol) applying four cycles of C_7 [18] during the excitation time $t_{\mathrm{exc}} =$ 0.8 ms for double-quantum preparation at a MAS spinning speed $\omega_R = 2\pi \times 10$ kHz. All ^{1}H DQ coherences within the monomeric unit of polybutadiene, shown in (b) are observed (c) in double-quantum spectrum measured at $T = 298$ K. The $CH=CH$ signal has its maximum intensity at the chemical shift of the *cis*-configuration due to lower proton distance, whereas the maximum intensity of the CH_2-CH coherence at the chemical shift of the *trans*-configuration reflects the higher order parameter of this configuration.

Data were obtained at $T = T_g + 50$ K $= 224$ K, the lowest temperature at which the MAS experiment can be safely performed. The absolute value of the S_i were obtained by two independent methods. First, we measured single-quantum ^{1}H MAS spectra; e.g., Fig. 2(b). The absolute value for the strongest dipolar coupling of the two protons in the CH_2 group can be obtained by an analysis of the spinning sideband pattern in terms of the spin

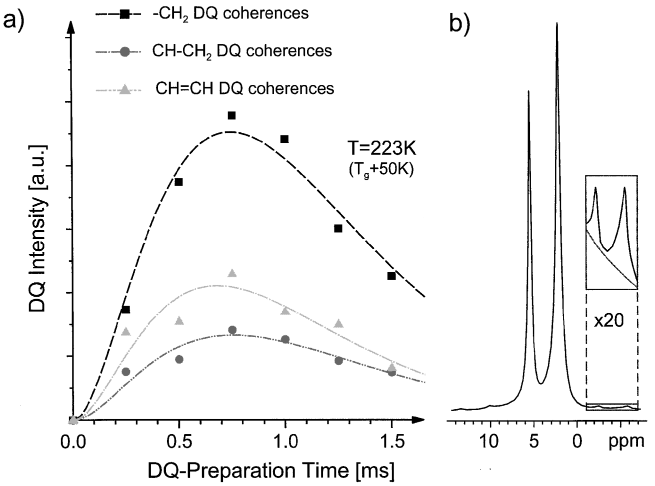

FIG. 2. (a) Relative dipolar couplings are extracted from a series of double-quantum spectra by fitting the time dependence of the double-quantum excitation for the different coherences. (b) The absolute value of the strongest dipolar coupling is determined from relative sideband intensities of ^{1}H MAS spectra, using a spinning frequency of $\omega_R = 2\pi \times 4$ kHz.

pair approximation [13,16]. Second, we determined the absolute value of an averaged overall dipolar coupling from the ratio of the intensity of a double-quantum filtered ($t_1 = 0$) signal, for short excitation times, to the intensity obtained in an analogous experiment, albeit without the selection of quantum coherence order. Within experimental uncertainties both results fully agree. The results are listed in Table I. From $S_{\mathrm{CH=CH}} = 0.13$ the order parameter of the double bond can be directly obtained by a simple projection procedure, yielding $S_{\mathrm{C=C}} \approx 0.20$.

Following Ref. [9] one may be tempted to relate the residual anisotropy to the restrictions due to the entanglements. Indeed, we find the initial residual coupling to be independent of molecular weight for $M_w \geq 4M_e$ and vanishing for $M_w \leq M_e$. Using the approximate relation $S \approx 3/(5N_k)$ (N_k denotes the number of Kuhn segments between two entanglements [14,20]) one obtains $S_{\mathrm{C=C}} = 0.028$ as an upper bound for the influence of the entanglements. This value is almost an order of magnitude smaller than the experimental value. Hence we have to conclude that the restrictions by the entanglements cannot be the only source for explaining the residual chain order. A possible reason for this strongly anisotropic rotational dynamics in PB may be the formation of significant intermolecular orientational correlations. Such local packing effects would strongly restrict the local degrees of freedom, leading to an anisotropic time averaged conformation. Indeed, such orientational correlations of adjacent polymer chains have been observed experimentally [21] as well as numerically [22], whereas this effect disappears for flexible chains as well as shorter chains [22]. In order to rationalize the relative values of the three different experimentally accessible order parameters, we averaged over all conformations of a part of a PB chain in agreement with its RIS statistics [19]. We required that the directions of the double bonds of the olefinic groups on average are loosely correlated with some arbitrary but fixed external direction representing the packing constraint corresponding to some local anisotropic potential. The degree of correlations has been adjusted such that on average $S_{\mathrm{CH}_2} = 0.06$ in agreement with experiment. Details of this calculation will be presented under separate cover [13]. The resulting order parameters are given in Table I. Within the range of uncertainty, they agree with the experimental values. The same calculation yields only a very small order parameter for the aliphatic C—H bonds, consistent with the narrow ^{2}H spectra observed in PB melts [23]. This emphasizes the advantage of our double-quantum technique, which determines the chain order from several proton pairs.

TABLE I. Measured and calculated order parameters for different atomic pairs of PB at $T = 224$ K. The calculations have been performed on the basis of the RIS model of PB. The experimental value of S_{CH_2} has been used as a basis for the simulations.

	$S_{-\mathrm{CH}_2}$	$S_{\mathrm{CH}_2-\mathrm{CH}}$	$S_{\mathrm{CH=CH}}$	$S_{\mathrm{C=C}}$	$S_{\mathrm{C-D}}$
Expt.	0.06	0.08	0.13	⋯	⋯
RIS Sim.	0.06	0.06	0.12	0.24	0.02

As mentioned above, translation of the chain will reduce the residual dipolar coupling leading to $C(t/t_e) < 1$. Here, t_e is proportional to the viscosity of short PB chains [24] and has been chosen to agree with the time a segment needs to move a typical distance between two adjacent entanglements as determined, e.g., from the mass dependence of the viscosity [20]. Scaling by $t_e(T)$ translates the temperature dependence into an effective time dependence. We measure between $T_g + 50$ K and $T_g + 120$ K, always choosing $t = 0.5$ ms. 2D double-quantum spectra recorded at various temperatures have shown that $C(t/t_e)$ is therefore sufficient. The results are shown in Fig. 3. From left to right the temperature increases. The accessible temperature range towards high temperatures is limited by the tendency of PB chains to crosslink. For all three molecular weights one clearly observes the reduction of the dipolar couplings.

For a better understanding of the observed time dependence as well as the mass dependence we first compare the data with the predictions of the standard reptation model [2]. We assume that the local constraints, i.e., the entanglements in the framework of the reptation model, do not change with time. Then $C(t/t_e)$ can be directly interpreted as the probability that a segment after time t/t_e is between the same two entanglements as for $t = 0$. It does not matter whether or not the segment has experienced different parts of the tube in between. Hence $C(t/t_e)$ is interpreted as a return-to-origin probability. As shown in Ref. [9] one then expects three time regimes: $C(t/t_e) \propto t^{-1/4}$ ($t < t_c$), $C(t/t_e) \propto t^{-1/2}$ ($t_c < t < t_d$), and $C(t/t_e) \propto \exp(-t/t_d)$ ($t > t_d$), where $t_c \equiv \pi t_r$ and

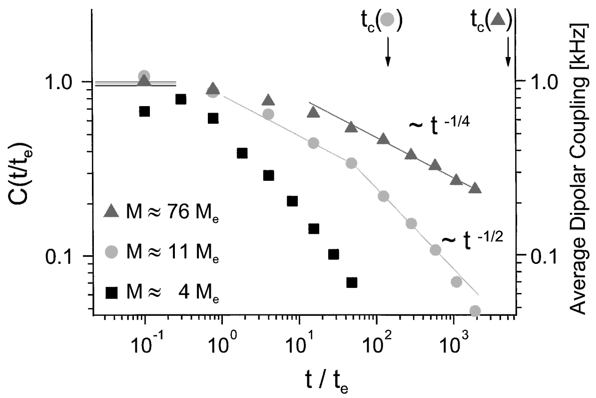

FIG. 3. Temperature dependent double-quantum filtered measurements probe the translational motion of polybutadienes with different molecular weights. The known temperature dependence of $t_e(T)$ is used to obtain the time dependence of the local order parameter over four decades. The correlation function $C(t/t_e)$ as well as the residual dipolar coupling of the CH_2 group are displayed. Two observed power laws are indicated.

t_d denotes the terminal relaxation time of the tube [2,13]. The exponents basically reflect the corresponding exponents of the mean square displacement. Furthermore, one expects that $C(t/t_e)$ does not depend on Z for $t < t_c$.

For $Z = 11$ or $Z = 76$ our data are in agreement with the predicted time dependences. Furthermore, for $Z = 11$ the estimated crossover time t_c corresponds well with the experimental observation [2]. However, the significant Z dependence of $C(t/t_e)$ for $t < t_c$ disagrees with the theoretical predictions. Qualitatively, the decay of $C(t/t_e)$ occurs earlier than expected which is especially pronounced for $Z = 4$.

These deviations may be related to the fact that the assumption of static local constraints does not hold for small Z. In the framework of the reptation model the local constraints relax on a time scale of t_d. Since $t_c/t_d \propto 1/Z$ the local tube stability for $t = t_c$ is smaller for shorter chains. Hence only for large Z we can expect that $C(t/t_e)$ reflects translational dynamics, which would, in principle, also be determined by pulsed field gradient NMR in extremely high field gradients [25]. Our experiment, however, primarily monitors reorientational dynamics, Eq. (1), and thus contains additional information about the stability of the local packing.

In fact, comparison with the reptation model is complicated, because the very large order parameter of PB (see above) is not predicted by the simple tube concept and may give rise to further unforeseen effects. Moreover, the modecoupling theory of the polymer dynamics predicts a significant Z dependence for the mean square displacement even for very large Z values [26]. It would be interesting to see whether the significant Z dependence of our rotational observable could be reproduced by this modecoupling approach.

In summary, we have measured the chain dynamics of a PB polymer melt well above the glass transition via double-quantum NMR. First, we observed that the absolute values of the local residual order parameters are significantly larger as implied by a simple picture relating the local constraints exclusively to some kind of entanglements. Second, we determined on a molecular scale the time dependence of the chain relaxation. In contrast to pure measurements of the mean square displacement our results also allow one to analyze the long-time stability of local constraints. The experimental data indicate that this stability strongly depends on the molecular mass. Clearly, more systems need to be studied in order to clarify the nature of these time-dependent ordering effects in terms of chain structure and molar mass.

We gratefully acknowledge stimulating discussions with I. Schnell, D. E. Demco, U. Wiesner, P. Sotta, and M. Fuchs and financial support by the SFB 262 (Deutsche Forschungsgemeinschaft).

[1] P. E. Rouse, J. Chem. Phys. **21**, 1272 (1953).
[2] M. Doi and S.F. Edwards, *The Theory of Polymer Dynamics* (Clarendon, Oxford, 1986).
[3] P.-G. de Gennes, J. Chem. Phys. **55**, 572 (1971).
[4] K. S. Schweizer, J. Chem. Phys. **91**, 5822 (1989).
[5] B. Ewen, D. Richter, B. Farago, and U. Maschke, Progr. Colloid Polym. Sci. **91**, 121 (1993).
[6] D. Richter, L. Willner, A. Zirkel, B. Farago, L. J. Fetters, and J. S. Huang, Phys. Rev. Lett. **71**, 4158 (1993).
[7] M. G. Brereton, Macromolecules **22**, 3667 (1989).
[8] E. Fischer, R. Kimmich, and N. Fatkullin, J. Chem. Phys. **104**, 9174 (1996).
[9] R. C. Ball, P. T. Callaghan, and E. T. Samulski, J. Chem. Phys. **106**, 7352 (1997).
[10] K. Kremer and G. S. Grest, J. Chem. Phys. **92**, 5057 (1990).
[11] J. Collignon, H. Sillescu, and H. W. Spiess, Colloid Polym. Sci. **259**, 220 (1981).
[12] K. Schmidt-Rohr and H. W. Spiess, *Multidimensional Solid State NMR and Polymers* (Academic, London, 1994).
[13] R. Graf, A. Heuer, and H. W. Spiess (to be published).
[14] J. P. Cohen Addad, Prog. Nucl. Magn. Reson. Spectros. **25**, 1 (1993).
[15] M. Munowitz and A. Pines, Adv. Chem. Phys. **66**, 1 (1987).
[16] J. Gottwald, D. E. Demco, R. Graf, and H. W. Spiess, Chem. Phys. Lett. **243**, 314 (1995).
[17] R. R. Ernst, G. Bodenhausen, and A. Wokaun, *Principles of Nuclear Magnetic Resonance in One and Two Dimensions* (Oxford University Press, Inc., Oxford, 1994).
[18] Y. K. Lee, N. D. Kunur, M. Helmle, O. G. Johannessen, N. C. Nielsen, and M. H. Levitt, Chem. Phys. Lett. **242**, 304 (1995).
[19] Y. Abe and P. J. Flory, Macromolecules **4**, 219 (1971).
[20] J. D. Ferry, *Viscoelastic Properties of Polymers* (John Wiley & Sons, Inc., New York, 1980), 3rd ed.
[21] C. A. Klug, W. Zhu, K. Tasaki, and J. Schaefer, Macromolecules **30**, 1734 (1997).
[22] A. Kolinski, J. Skolnick, and R. Yaris, Macromolecules **19**, 2550 (1986).
[23] A. Dardin, R. Stadler, Ch. Boeffel, and H. W. Spiess, Makromol. Chemie **194**, 3467 (1993).
[24] G. C. Berry and T. G. Fox, Adv. Polym. Sci. **5**, 261 (1968).
[25] G. Fleischer and F. Fujara, Nucl. Magn. Reson. Basic Princ. Prog. **30**, 159 (1994).
[26] K. S. Schweizer, M. Fuchs, G. Szamel, M. Guenza, and H. Tang, Macromol. Theory Simul. **6**, 1037 (1997).